

Collective Oscillations of Vortex Lattices in Rotating Bose-Einstein Condensates

T. Mizushima,¹ Y. Kawaguchi,² K. Machida,¹ T. Ohmichi,² T. Isoshima,³ and M. M. Salomaa³¹Department of Physics, Okayama University, Okayama 700-8530, Japan²Department of Physics, Graduate School of Science, Kyoto University, Kyoto 606-8502, Japan³Materials Physics Laboratory, Helsinki University of Technology,
P. O. Box 2200 (Technical Physics), FIN-02015 HUT, Finland

(Dated: January 8, 2002)

The whole collective excitation spectrum with low energies for vortex lattices is studied in rotating Bose-Einstein condensates by solving Bogoliubov-de Gennes (BdG) equation, including the Tkachenko mode observed recently at JILA. We classify these modes into three categories; transverse shear, comm on-longitudinal, and differential longitudinal modes. We also solve the time-dependent Gross-Pitaevskii (TDGP) equation to simulate the actual JILA experiment, yielding the Tkachenko and other two breathing modes. Combination of two methods on BdG and TDGP allows to unambiguously identify all observed modes.

PACS numbers: 03.75.Lm, 05.30.Jp, 67.40.Vs

Because of its fundamental significance in superfluidity the quantized vortex has attracted much attention on various fields ranging from superconductors, superfluid ³He, ⁴He to neutron stars [1]. Recently in dilute alkali atom gases, vortices have been created by three different means, phase imprinting [2], topological phase engineering [3] and optical spoon stirring [4]. The former two are predicted theoretically [5, 6] prior to experiments. Several experimental groups are now able to prepare a vortex array with hundreds of vortices routinely in harmonically trapped Bose-Einstein condensates (BEC).

In mid 1960' Tkachenko [7] predicts that a vortex lattice can sustain collective vortex oscillation in which the vortex cores move mainly transversally to its propagation direction around the equilibrium position. Subsequent theoretical developments are made by Baym and Chandler [8], Williams and Fetter [9] and others [10] (See for review, Refs. [1, 11]). In superfluid ⁴He the Tkachenko mode is observed in 1982 [12].

Recently, Coddington et al. [13] have succeeded in observing the Tkachenko mode (TK) in rotating BEC of ⁸⁷Rb. The TK wave is excited by removing the condensates of the central region of the rotating cloud. They create the lowest and second lowest TK modes and measure their energies $\epsilon_{(1,0)}$ and $\epsilon_{(2,0)}$ as a function of the rotation frequency Ω . Also they provide various fundamental properties, some of which are explained by Anglin and Caccioppo [14], and Baym [15]. These theories extend the previous hydrodynamic description for infinite systems to a finite harmonically trapped system.

Here we take a different approach to this problem: We wish to fully understand low-lying collective excitation structure of trapped BEC, not only TK mode, but also other important modes and their internal relationship. We have to construct a first principles theory, namely Bogoliubov-de Gennes equation (BdG) coupled with the Gross-Pitaevskii equation (GP). The set of equations within the Bogoliubov framework is regarded

as most microscopic theory for present dilute Bose gases in the sense that there is no adjustable parameter once we fix the atom species and atom number, etc. Thus it is quite reasonable to expect that this framework must work well for analyzing the TK mode and provide also full spectral feature of the low energy excitations free from the limitations of hydrodynamics, which was only way to describe the TK mode so far. Then we will be able to better characterize various modes, such as anticipated three kinds of the compressional modes, transverse, comm on longitudinal and differential longitudinal waves. These are characteristic in two component system of the vortex lattice and superfluid. Some of the selected comm on longitudinal modes in a vortex lattice (breathing and quadrupole modes) are examined recently [16, 17] within hydrodynamics. To our knowledge, this kind of microscopic theory has not been worked out to exhaust the whole spectrum, partly because, we think, there is no appropriate system to urge it. This theory might be useful to understand the related problems, such as vortex pinning or vortex melting in a superconductor which are analyzed only phenomenologically.

In a rotating frame with the rotation frequency Ω , the time-dependent Gross-Pitaevskii equation (TDGP) is written for the condensate wave function ψ as

$$i\hbar \frac{\partial \psi}{\partial t} = \frac{\hat{p}^2}{2m} + V_e(\mathbf{r}; \Omega) + g|\psi|^2 \psi; \quad (1)$$

where $\hat{p}(\mathbf{r}) = i\hbar \nabla - m \hat{\mathbf{z}} \times \mathbf{r} \Omega$ and the effective confining potential $V_e(\mathbf{r}; \Omega) = \frac{1}{2}m(\dot{r}^2 - \Omega^2 r^2)$ with the radial trap frequency \dot{r} .

In order to study the collective oscillations of vortex lattices microscopically, we first consider the equation of motion for the small perturbation around the stationary state ψ_0 , i.e., $\psi(\mathbf{r}; t) = \psi_0(\mathbf{r}) + u_q(\mathbf{r})e^{i\mathbf{q} \cdot \mathbf{r} + i\epsilon_q t} + v_q(\mathbf{r})e^{i\mathbf{q} \cdot \mathbf{r} + i\epsilon_q t}$, where the equilibrium state ψ_0 is determined by the stationary GP equation. By retaining terms up to first order

in u and v , we derive the BdG equation:

$$\begin{pmatrix} L(r; \omega) & g \frac{\partial}{\partial r}(r) \\ g \frac{\partial}{\partial r}(r) & L(r; \omega) \end{pmatrix} \begin{pmatrix} u_q(r) \\ v_q(r) \end{pmatrix} = \hbar \omega \begin{pmatrix} u_q(r) \\ v_q(r) \end{pmatrix}; \quad (2)$$

where $L(r; \omega) = \hat{p}^2(r) = 2m + V_e(r; \omega) + 2g|g(r)|^2$. We take up the JILA experiment on 2.0×10^6 ^{87}Rb atoms confined in a trap with the radial frequency $\omega_r = 8.3$ Hz and the axial one $\omega_z = 5.2$ Hz [13]. Assuming their system as a two-dimensional geometry at high rotation frequencies, we introduce the linear density $n_z(r)$ along the z axis. The equilibrium state g therefore must satisfy the normalization condition $n_z(r) = \int_{\mathbb{R}^2} |g|^2 dx dy$. By the Thomas-Fermi (TF) theory and the assumption of the solid-body rotation [18], one obtains the relation: $n_z(r) = R_{TF}^4 = 16ad_x^4$, where a is a s-wave scattering length, $d_x^2 = \hbar^2 / (2m \omega_r^2)$, and R_{TF} is the radius estimated by TF approximation. We discretize the two-dimensional space into typically $300^2 \times 1000^2$ mesh to solve TDGP and BdG equations.

Here, since we consider the vortex array with the six-fold symmetry, the wave function of the stationary state has the relation, $g(R^n r) = g(r)e^{in\theta} = e^{i3\theta}$, where we introduce the rotation $n=3$ (n integer) around the center of the trap, $R^n r$. We then obtain the following relation from Eq. (2): $u_{q,m}(R^n r) = u_q(r) \exp \frac{in}{3} (m+1)$ and $v_{q,m}(R^n r) = v_q(r) \exp \frac{in}{3} (m-1)$, where $m = 0; 1; 2; 3$. In order to classify the low-lying collective excitations, we introduce the following quantity, $F_q^{(u)}(m) = \int_{\mathbb{R}^2} dr u_q(r) \int_{\mathbb{R}^2} u_{q,m}(R^n r) = \int_{\mathbb{R}^2} dr [j_r(r)^2 + j_\theta(r)^2]$. Furthermore we define the average angular momentum as $q = \int_{\mathbb{R}^2} \hbar L_z i_u + \hbar L_z i_v = \int_{\mathbb{R}^2} \hbar L_z i_g = \int_{\mathbb{R}^2} dr [j_r(r)^2 + j_\theta(r)^2]$, where $\hbar L_z i_g = \int_{\mathbb{R}^2} i dr g \hat{L}_z g = \int_{\mathbb{R}^2} dr j_g^2$, and $\hbar L_z i_u = \int_{\mathbb{R}^2} i dr \hat{L}_z u$ [19]. In the axisymmetric situation, m and q reduce to the same integer quantum number.

The low energy excitations are shown in Fig. 1 where the vortex configuration in the equilibrium is displayed in Fig. 1(a). A regular triangular lattice is formed by 37 vortices at $\omega = 0.7\omega_r$. In Fig. 1(b), the excitation energy up to $\omega = 3.5\omega_r$ is shown as a function of the average angular momentum q . Each collective mode is classified by the additional quantum number m obtained from the above condition, $F_q(m)$, which characterizes the oscillation pattern. For example, breathing (BR), dipole (DP), and quadrupole (QP) modes have $m = 0, 1, 2$ respectively. The branch extending towards the larger q from the origin consists of the surface modes which are periodically placed with $m \pmod{6}$, where the outer condensate surface oscillates, almost keeping the vortex cores still at the equilibrium position. The other branch situated at higher energy starting at $\omega = 2\omega_r$ is also another type of the surface modes which have a node along the radial direction. The energy spectrum of the lower modes is depicted in Fig. 1(c) where the lowest TK and the second lowest TK are embedded among other vortex core precession modes. The lowest mode $\omega =$

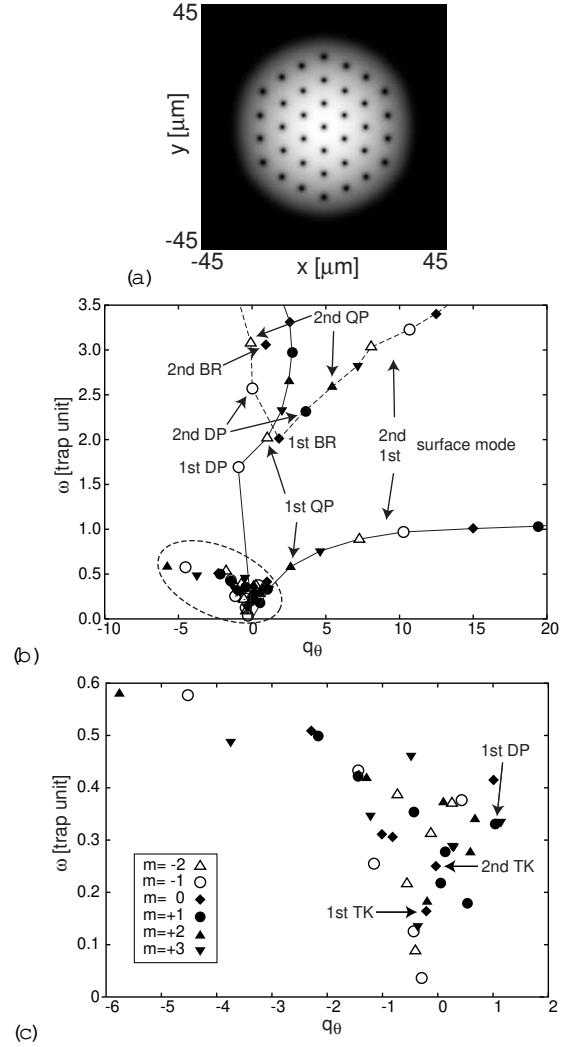


FIG. 1: Density profile of the condensate with 37 vortices at $\omega = 0.7\omega_r$. (a). Collective excitations up to $\omega = 3.5\omega_r$ (b) and the lower excitations marked by the dotted line are shown in (c) as a function of q . The all modes are classified by the another quantum number m .

$0.036\omega_r$ with $q = 0.3$ and $m = 1$ describes a motion where the vortex cores precess around the equilibrium position with the same phase as a whole. This is also the case for rotations.

In Fig. 2, we illustrate the oscillation patterns for selected collective modes obtained from the linear fluctuation $(r; t)$: The lowest TK mode $(1, 0)$ is shown in Fig. 2(a) where the empty (filled) circle indicates the equilibrium (the quarter-period) position of the vortex core. The line is a fitted sinusoidal modulation wave (the amplitude is exaggerated). It is seen that the modulation has a node at $r_{\text{node}} = 0.64R_{TF}$, which is in good agreement with the JILA data $r_{\text{node}} = 0.665R_{TF}$. The second TK mode $(2, 0)$ is shown in Fig. 2(b). It is seen that in contrast with the first TK mode whose core modulation

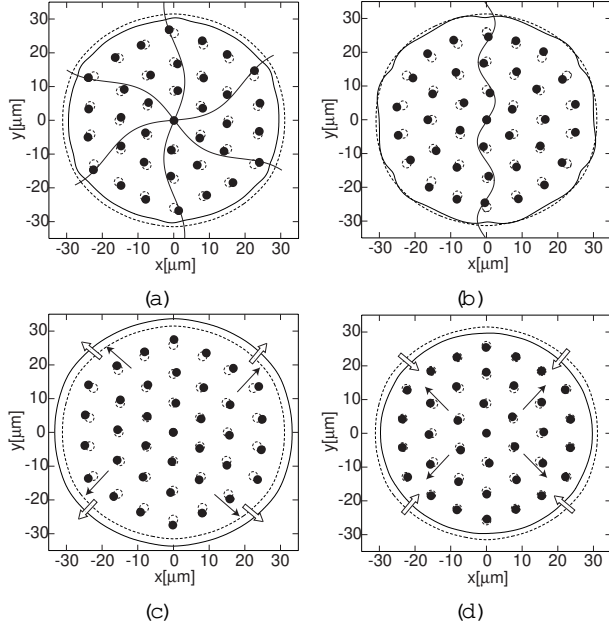


FIG. 2: Oscillation patterns for the lowest TK (a), the second TK (b), the lowest BR (c), and the second BR mode (d) are shown by the filled circles and the solid lines. The empty circles and dotted lines correspond to the equilibrium state.

is almost purely transverse, the second TK contains the longitudinal component in addition to the transverse one. Thus the resulting core motion is elliptic around the equilibrium position. This tendency coincides with the general expression for the ellipticity of the TK mode, namely the amplitude ratio of the longitudinal and transverse components $\alpha_L = \alpha_T / 1 = k_{TK}$ (k_{TK} : the wave length of the TK) [1], thus, the second TK with the shorter k_{TK} exhibits the larger longitudinal motion. We point out that by seeing the condensate radius in Fig. 2 (a) and 2 (b) the TK modes accompany the condensate fluid motion. It is also noticed that the ratio of the energies of these 1st ($(1;0)$) and 2nd ($(2;0)$) TK modes is $E_{(2;0)} / E_{(1;0)} = 1.56$ at $\mu = 0.71$, which is favorably compared with the experimental data 1.8 ± 0.2 at $\mu = 0.951$ [13] and with 1.63 by Anglin and Caccioppo [14]. The latter asserts that it is independent of μ .

As a typical mode other than TK, we take up here two contrasting compressional modes belong to the so-called breathing mode with the totally symmetric $m = 0$. In Figs. 2 (c) and 2 (d) the oscillation patterns of the first lowest BR mode and the second lowest BR mode depicted in Fig. 1 (b). The former (latter) BR mode is the in-phase (out-of-phase) motion between the cores and the condensates as seen from the two parallel (opposite) arrows in the figure. The inner (out) arrow denotes the motion of the cores (condensates). Therefore the former belongs to the common longitudinal mode while the latter to the differential longitudinal mode. It should be pointed out

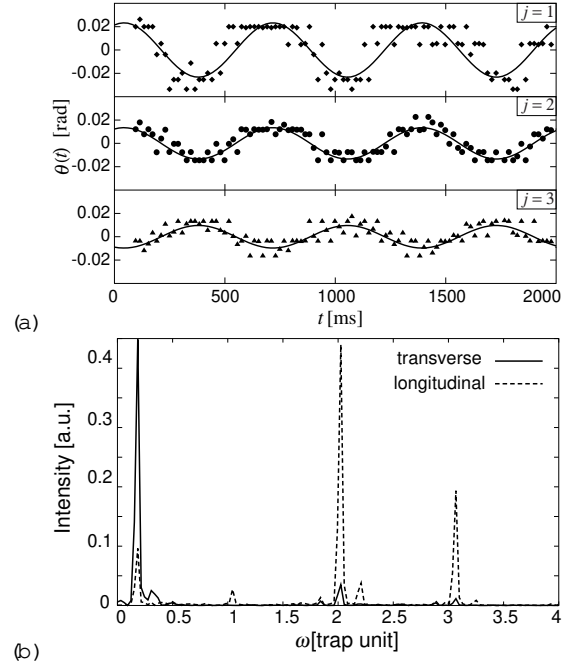


FIG. 3: In (a), transverse oscillations of vortices on three concentric circles are shown ($j = 1; 2; 3$ from trap center). The Fourier analysis of these oscillation patterns $\theta_j(t)$ and the longitudinal vortex motion $x_j(t)$ are depicted in (b).

that the inner core motion in Fig. 2 (c) and 2 (d) is rather transverse, meaning that even in nominally longitudinal BR mode all the vortex motion is not necessarily longitudinal. This might be related to the 'b-bending' in the third mode observed [13] as mentioned below.

Having studied all the low-lying excitations, let us now attempt to extend the analysis in the linear response regime into the non-linear dynamics with the real time evolution by simulating the TDGP (Eq. (1)). Since Codrington et al. excite TK mode by shining resonance laser on BEC center and produce inward flow, we introduce a Gaussian potential localized in the center of the trap, $V(r) = \frac{1}{2} \mu_e r^2 / R^2$ with $R = 0.5 R_{TF}$ in a certain period and watch the time evolution according to Eq. (1).

We show the resulting oscillation patterns and the Fourier analyses in Fig. 3. At $\mu = 0.71$, 37 vortices shown in Fig. 1 (a) form a concentric regular lattice around the central vortex, consisting of three concentric circles ($j = 1; 2; 3$ from the center). We analyze the transverse vortex motion for the vortex $\mathbf{r}_{jm}(t) = (x_{jm}(t); y_{jm}(t))$ in terms of the average angle defined by $\theta_j(t) = \frac{1}{6} \sum_{n=0}^5 [\arctan(y_{jm}(t)/x_{jm}(t)) - \arctan(y_{jm}(0)/x_{jm}(0))]$ where n denotes the vortices aligned along the line making the angle $n\pi/3$ from the vertical line (see Fig. 1 (a)). It is seen from Fig. 3 (a) where we plot the time dependence of the vortex motion for each circle ($j = 1; 2; 3$) that (1) there exist several oscillations superposed. (2) The most slow variation cor-

responding to the TK shows quite sinusoidal patterns for outer vortices of $j = 2$ and 3 while the inner vortices exhibit a distorted non-linear wave form. (3) The outer vortices $j = 3$ is the anti-phase with the inner vortices $j = 1$ and 2. This coincides with the above calculation based on BdG. In fact the nodal position for both calculations agree each other.

In Fig. 3(b), the Fourier analysis of these transverse oscillations, $\psi_j(t)$, and the longitudinal vortex oscillations, $r_j(t)$, is depicted; It is seen that the sharp peak at $\omega = 0.18!_r$ precisely corresponds to the first TK mode $!(1,0)$ identified before (see Fig. 1(c)). The several higher harmonics for $j = 1$ matches with the above fact (2). The second peak at $\omega = 2.0!_r$ corresponds to the first BR mode belonging to the common-longitudinal mode. The third peak at $\omega = 3.1!_r$ can be identified to the second BR mode (see Fig. 1(b) and 2(d)) as the differential longitudinal mode. These three oscillations nicely match with observed characteristics. In particular, the third mode which was tentatively assigned as higher-order hydrodynamic mode due to an anharmonic radial potential by Cozzini and Stringari [16] is now identified as above.

In Fig. 4 we plot the first TK energy $!(1,0)$ as a function of $\omega = !_r$ together with the experimental data [13] and the hydrodynamic prediction by Anglin and Caccioppo [14]. The overall tendency between our results and the data coincides each other in a quantitative level. We emphasize that our calculation contains no adjustable parameter and also that the two results with BdG and TDGP agree within the numerical accuracy when they overlap below $0.8!_r$, beyond which BdG can not be feasible. The inset of Fig. 4 shows the ω -dependence of the first and second BR modes. It is known that the former is consistent with the earlier prediction by Pitaevskii and Rosch [20], who point out that two-dimensional BR mode has the universal eigenfrequency $\omega = 2.0!_r$. Our result reproduces it and explains the observation mentioned above that the second peak in Fig. 3(b) indeed the first BR mode. As for the third peak in Fig. 3(b) identified as the second BR mode before, it is seen from this inset that the observed value $18.5 \pm 0.3 \text{ Hz}$ ($2.2!_r$) seems reasonable, judging from the overall ω -dependence towards ω_c .

In summary, we have examined the whole low energy excitation spectrum in a vortex lattice by solving BdG and classified these into three categories, transverse shear, common-longitudinal, and differential longitudinal modes. We have also succeeded in simulating the actual experiment to excite the TK mode by solving TDGP, identifying the other two modes.

During preparation of the manuscript, we learned of two closely related preprints [21] and [22]. The former (latter) treats BdG (TDGP) on the TK mode.

The authors thank V. Schweikhard, I. Coddington, and M. Ichio for useful discussion and/or communication. K.M. is grateful to G. Baym, J.R. Anglin, S. Stringari,

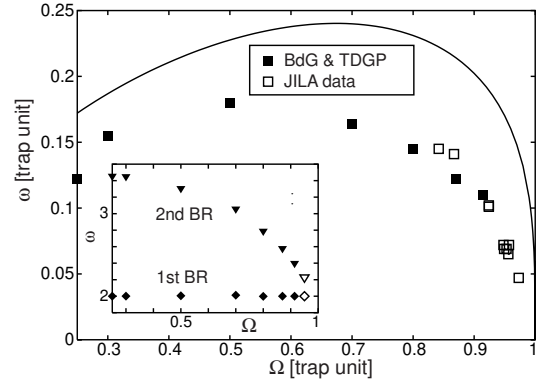


FIG. 4: The frequencies of three modes are compared with the JILA data (empty ones) as a function of Ω : The TK (filled squares) in the main panel, and in the inset the first BR (filled diamonds) and the second BR (filled triangles). The solid line presents the dispersion relation, $\omega = 1.43 \Omega$ [14].

and A.L. Fetter for useful and enthusiastic discussion on the Tkachenko mode at Aspen Center for Physics.

-
- [1] R.J. Donnelly, in *Quantized Vortices in Helium II* (Cambridge University Press, Cambridge, 1991).
 - [2] M.R. Matthews et al, *Phys. Rev. Lett.* **83**, 2498 (1999).
 - [3] A.E. Leanhardt et al, *Phys. Rev. Lett.*, **89**, 190403 (2002).
 - [4] K.W. Madison et al, *Phys. Rev. Lett.*, **84**, 806 (2000).
 - [5] J.E. Williams and M.J. Holland, *Nature* **401**, 568 (1999).
 - [6] M. Nakahara et al, *Physica B* **284-288**, 17 (2000); T. Isoshima et al, *Phys. Rev. A* **61**, 063610 (2000).
 - [7] V.K. Tkachenko, *Sov. Phys. JETP* **29**, 245 (1969) and earlier references therein.
 - [8] G. Baym and E. Chandler, *J. Low Temp. Phys.* **50**, 57 (1983); **62**, 119 (1986); G. Baym, *Phys. Rev. B* **51**, 11697 (1995).
 - [9] M.R. Williams and A.L. Fetter, *Phys. Rev. B* **16**, 4846 (1977).
 - [10] L.J. Campbell and R.M. Zi, *Phys. Rev. B* **20**, 1886 (1979); L.J. Campbell, *Phys. Rev. A* **24**, 514 (1981).
 - [11] E.B. Sonin, *Rev. Mod. Phys.* **59**, 87 (1987).
 - [12] C.D. Anderson and W.I. Glaberson, *J. Low Temp. Phys.* **48**, 257 (1982).
 - [13] I. Coddington et al, *cond-mat/0305008*.
 - [14] J.R. Anglin and M. Caccioppo, *cond-mat/0210063*.
 - [15] G. Baym, *cond-mat/0305294*.
 - [16] M. Cozzini and S. Stringari, *Phys. Rev. A* **67**, 041602 (2003).
 - [17] S. Choi et al, *cond-mat/0306549*.
 - [18] D.L. Feder and C.W. Clark, *Phys. Rev. Lett.* **87**, 190401 (2001).
 - [19] T. Isoshima et al, *cond-mat/0212528*.
 - [20] L.P. Pitaevskii and A. Rosch, *Phys. Rev. A* **55**, R853 (1997).
 - [21] L.O. Baksmaty et al, *cond-mat/0307368*.
 - [22] T.P. Simula et al, *cond-mat/0307130*.